Thermal Effects of Pressure Surge and Adiabatic Compression in the Priming of Propulsion and Propellant Transfer Systems

Max Kandula[1], Brian M. Nufer[2]
NASA Kennedy Space Center, Florida 32899

and

Graham K. Webster[3]
NASA Goddard Space Flight Center, Greenbelt, Maryland 20771

Surge pressures and adiabatic compression during priming of evacuated lines in propulsion and propellant transfer systems has been considered. Test data were obtained for desaturated and saturated water for surge pressures and adiabatic compression for various supply pressures and temperatures. Scaling of surge pressures at different temperatures has been carried out with the aid of Joukowsky model. The thermal effects associated with surge pressure and the attendant adiabatic compression have been investigated with the aid of a simplified analytical model, which represents an extension of the model developed by Lecourt and Steelant[1]. It has been shown that the predictions from the model compare satisfactorily with test data for a water/helium system, and existing test data for different liquid/gas combinations.

Nomenclature

c	=	sound speed
c_0	=	speed of sound in liquid
c_p	=	specific heat at constant pressure
D	=	tube internal diameter
E	=	Young's modulus of elasticity
m	=	mass
$\dot{m}$	=	mass flow rate
p	=	pressure
t	=	time
S	=	scale factor for peak surge pressure
T	=	temperature
t	=	time, also tube wall thickness
V	=	velocity
α	=	$\rho_g c_{pg} / \rho_l cp_l$
γ	=	specific heat ratio
μ	=	dynamic viscosity of fluid, also Poisson's ratio
ρ	=	density of fluid

[1]Technical Fellow, KBR, Mail Stop LASSO-001, Associate Fellow, AIAA
[2]Propellant Transfer Assembly Lead, Advanced Engineering Development, Mail-Stop NE-L5.
[3]Aerospace Technologist Aerospace Propulsion Systems, Propulsion, Mail Stop 597, Member, AIAA

Subscripts

ad	=	adiabatic
eq	=	equilibrium
g	=	gas
l	=	liquid
0	=	initial state
WH	=	water to hydrazine (scaling)

I. Introduction

When propellant is primed into evacuated manifolds (or manifolds containing a low-pressure gas-vapor mixture) of propulsion subsystem and propellant transfer subsystems (client side), flash boiling occurs near the propellant front, generating vapor bubbles (Bombardieri et al.[2]). Dissolved pressurant gas (GHe, GN2, etc.) is concurrently released, generating gaseous bubbles. Thus, in general, priming is accompanied by both vapor cavitation and gaseous cavitation. When the pressure rises downstream of the system's cavitating venturi throat (pressure recovery region), some of the gas bubbles will collapse and be reabsorbed. The absorption process is known to be slow relative to desorption (Bombardieri et al.[2]).

Adiabatic compression during priming of evacuated lines has been analyzed. The associated thermal effects due to pressure surges have been investigated with the aid of a simplified model. Predictions from the model have been compared with existing test data for different liquid/gas combinations.

II. Physical Processes of Surge Pressure and Adiabatic Compression

Figure 1 shows a schematic of compression when a high-pressure liquid travels through a nearly evacuated gaseous manifold region. The temperature of the vapor-gas mixture increases due to adiabatic compression (Valencia-Bell[2]). The direct contact between the propellant and vapor-gas mixture results in a liquid temperature well below the adiabatic compression temperature of the vapor/gas mixture on account of intense mixing and heat exchange in combination with the high thermal capacity of the propellant.

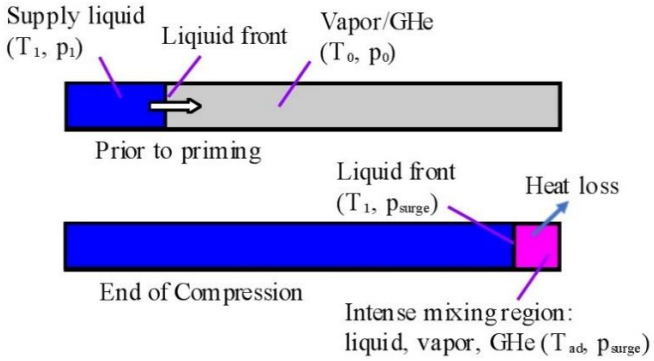

Fig. 1 Surge pressure and adiabatic compression during priming (adapted from Valencia-Bel[3]).

III. Analysis

A. Physical Assumptions

1. The propellant manifolds are assumed to be initially at near vacuum conditions (corresponding to an empty client propellant tank and depressurized manifolds). The vacuous manifold represents the worst case initial

condition for adiabatic compression. Higher gas/vapor pressure or the presence of liquid propellant in the manifold being primed would reduce adiabatic heating.
2. The pressure in the line manifold corresponds to vapor pressure of hydrazine at the prevailing initial temperature. This expectation is consistent with the GSFC test data[4] on internal depressurization of water.
3. The surge pressure is obtained from scaled water test data in accordance with the simplified Jowkowsky equation.
4. The heat loss from the system is neglected. This assumption is justified since the time scales (durations) for surge pressure and compressive heating are relatively small (order of a second or so).
5. The complex effects of bends, fittings, and flex hoses are neglected in the simplified model. In actuality, for example, flexhoses might act as surge pressure suppressors.

B. Simplified Model for Surge Pressure

A simplified model has been considered for estimating the surge pressures occasioned near the end of the line. The surge pressure is expressed by

$$p_{\text{surge}} = p_{\text{tank}} + \Delta p_{\text{surge}} \tag{1a}$$

where the surge pressure differential is expressed by the Joukowsky equation (Joukowsky[5])

$$\Delta p_{\text{surge}} = \rho c V \tag{1b}$$

In Eq. (1b), ρ is the fluid density (990 kg/m^3 for hydrazine at 25 deg C), c is the speed of sound (2074 m/s for hydrazine at 25 deg C), and ΔV is change in the flow velocity. For initially stagnant conditions in the line, $\Delta V = V$. The presence of bubbles in the liquid column in the line likely helps decrease the surge pressure through a decrease in speed of sound.

The sound speed, considering tube elasticity, is obtained from the relation (Prickett et al.[5])

$$c = \frac{c_0}{\sqrt{1 + \dfrac{\rho c_0^2}{E}\left(\dfrac{D}{t}\right)\left(\dfrac{5}{4} - \mu\right)}} \tag{1d}$$

where c_0 is the speed of sound in liquid, ρ is the liquid density, E is the Young's modulus of elasticity, D is the tube internal diameter, t is the tube wall thickness, μ is Poisson's ratio.

In the present analysis, the estimated surge pressure based on Joukowsky equation is considered (assumed) independent of the downstream volume.

Surge Pressure Scaling Based on Joukowsky's Equation

Assuming that the line pressure is negligible compared to the supply pressure, the surge pressure scale factor from fluid 1 (substitute) to fluid 2 (actual propellant), S_{12}, is determined from[6,7]

$$S_{12} = \frac{(\Delta p)_{\text{surge},2}}{(\Delta p)_{\text{surge},1}} = \frac{\left(\sqrt{\rho c}\right)_2}{\left(\sqrt{\rho c}\right)_1} \tag{2}$$

In summary, the basic surge pressure is evaluated from the Joukowsky equation. Elasticity effects on the surge pressure through the speed of sound are also considered. The scale factor for surge pressure from water to hydrazine is accordingly determined.

C. Model for Adiabatic Compression

A simple model has been considered for predicting the propellant temperature rise caused by the adiabatic compression that results from peak surge pressures (Lecourt and Steelant[1]). The peak surge pressures are based on simplified estimates in accordance with Joukowsky equation (1b). The finite velocity of the liquid-vapor/gas front (direct contact) approaching the primed manifold tubing end results in intense mixing and heat transfer between the liquid and the gas. This intense mixing helps reduce the liquid temperature significantly.

An energy balance yields

$$m_g c_{pg2}\left(T_{g2} - T_{\text{eq}}\right) = m_l c_l \left(T_{\text{eq}} - T_l\right) \tag{3}$$

where T_{g2} is the adiabatic compression temperature of gas, T_{eq} is the equilibrium temperature, m_g is the mass of the gas in the stagnation region, m_l is the mass of liquid, c_{pg2} is the specific heat of gas at T_{g2}, and c_l is the specific heat of liquid. The adiabatic compression temperature of gas is determined from the adiabatic law:

$$T_{g2} = T_{g1}\left(p_{g2} / p_{g1}\right)^{(\gamma-1)/\gamma} \tag{4}$$

where p_{g1}, p_{g2} refer to the initial and final pressure of the gas, respectively. This equation assumes that no appreciable heat transfer to the fluid system walls takes place during compression. If the pressure rise is slow (that is, the flow velocity in the flow line is small), then there would be heat transfer to the fluid system walls and the peak gas temperature due to compression will be reduced. Note, however, that even if the compression process is slow, the heat transfer to the system will be negligible if the fluid system walls are sufficiently insulated.

The equilibrium liquid temperature is estimated from

$$T_{\text{eq}} = \frac{\alpha T_g + T_l}{1+\alpha} \tag{5a}$$

where

$$\alpha = \rho_g c_{pg} / \rho_l c_{pl} \tag{5b}$$

Here, ρ_l, ρ_g refer to the density of liquid and gas, respectively. Eqn. (5a) represents the primary basis with which analytical results will be compared with the test data. The equilibrium (peak) liquid temperature is considerably smaller than the adiabatic compression (gas) temperature.

In view of the large temperature range of gas, the variation of density and specific heat should be taken into account since these two properties can vary significantly with temperature changes. In the present model, the density and specific heat of the compressed gas/vapor is evaluated at the average temperature (between the initial temperature and the final temperature of the gas after compression).

The present model for adiabatic compression has been validated by a comparison with existing test data for different fluid combinations. See Appendix 1 for details.

IV. Test Setup

Figure 2 shows the schematic of the test set up. A typical on-orbit satellite refueling transfer manifold formed a basis for the water test setup. Test data for surge pressures were obtained in 2019-2021 in the KSC water test facility (considering water as simulant for hydrazine in flight). The surge pressures are measured by PT (low-speed) and HPT (high-speed) pressure transducers. The adiabatic compression temperature is measured by TT-15 (tubing skin-

mounted thermocouple) and TT-20 (internal probe) sensor. Surge pressure and adiabatic compression temperature data were obtained for both desaturated and saturated water.

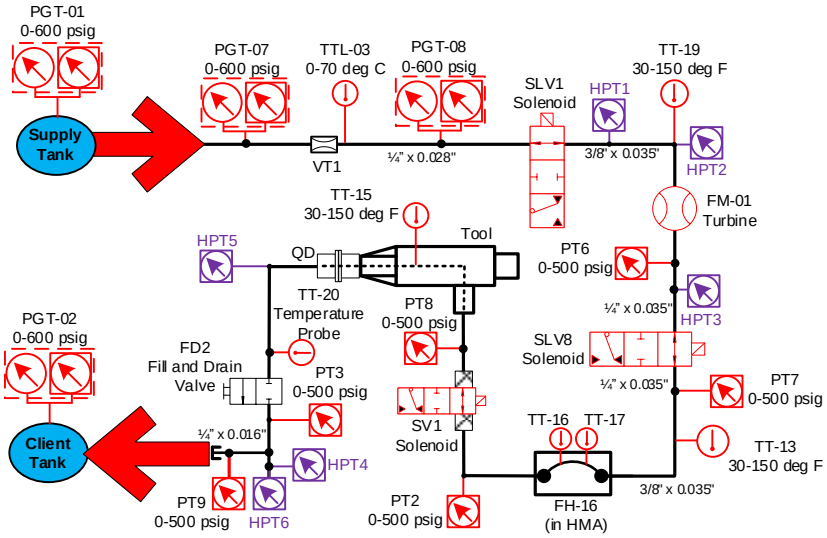

Fig. 2 Schematic of the instrumentation for pressure surge.

Figure 3 shows a photograph of the test setup. The priming volume is shown by the thick blue, green, and red lines. The locations of the various pressure transducers are indicated. Solenoid valves (SV1, SV2), along with two additional solenoid valves (SLV1, SLV8) to simulate latch valves, are also installed. The test set up reflects a servicer manifold volume of 310 to 345 cc (large and small volume), and a client manifold volume of 35 to 40 cc. Typical propulsion systems may vary in their internal volume; however, the model is independent of the volume, and is dependent upon the tubing inner diameter, wall thickness and material.

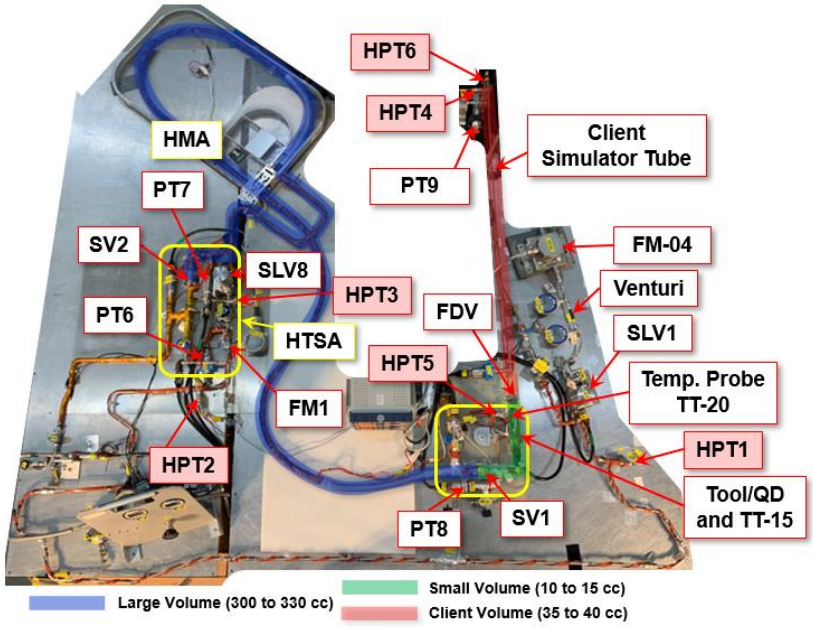

Fig. 3 Photograph of the test setup.

V. Results

A. Surge Pressures and Adiabatic Compression at 150 psig Supply

1. *Comparison of Surge Pressures in Desaturated and Saturated Water*

A direct comparison of the measured surge pressure history for the desaturated and saturated cases (as measured by HPT5 transducer) is displayed in Fig. 4. The peak surge for the saturated case is lower than that for the desaturated case. Also, the rate of rise of the surge pressure for the saturated case is lower than that for the desaturated case. This behavior is perhaps attributable to a larger release of GHe during priming with a saturated supply (which acts as a surge arrestor). Similar trends were experimentally reported by Lema et al.[8] using water-GN2 system. However, Bombardieri et al.[2] show data that is contrary to the present trends. See Appendix B for more details.

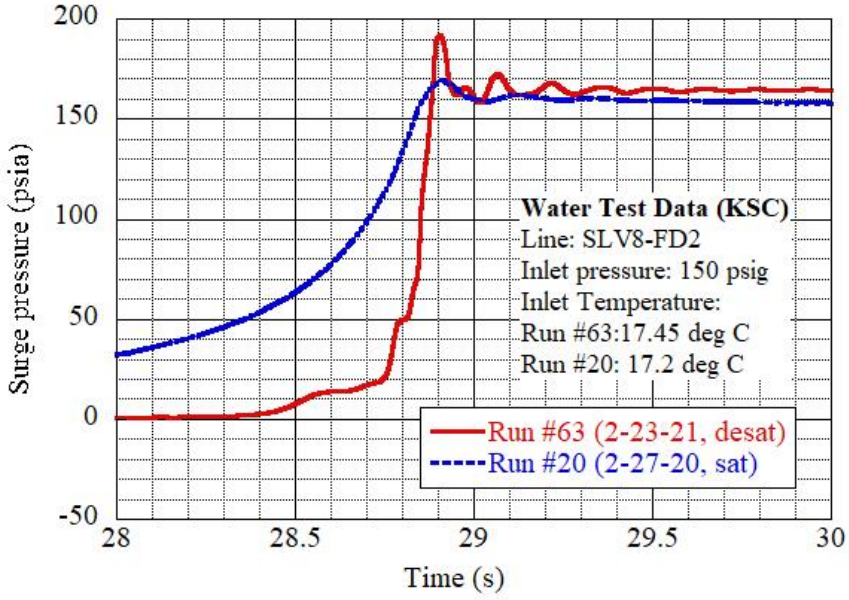

Fig. 4 Comparison of measured surge pressure history for desaturated and saturated water at a supply pressure of 150 psig.

2. *Self-Scaling for Water Surge Pressure*

Figure 5 presents the predicted self-scaling factor (or same-fluid temperature scaling factor) for water surge pressure at 150 psig (164.7 psia) supply based on the measured surge pressure at a reference temperature of 20 deg C. The reference condition at 20 deg C is indicated by the purple dot, and the prediction is shown by the solid red curve. The reference condition refers to the line volume (SLV1 to Client) with an average surge pressure between Runs #26 and #28. Based on the water test data at 20 deg C, the self-scaling factor for water is obtained for a temperature range of interest (10 to 40 deg C). Note that the test data for Run #63 corresponds to a different priming line (SLV8-FD2) with a volume differing from that of Runs #26 and #28. The predicted scale factor is found to be only weakly dependent on temperature and is found to increase slightly with supply liquid temperature. Since the tests in general show that the surge pressure is weakly dependent on the priming volume, the predicted solid curve is expected to hold with reasonable accuracy for a range of priming (manifold) volumes considered here.

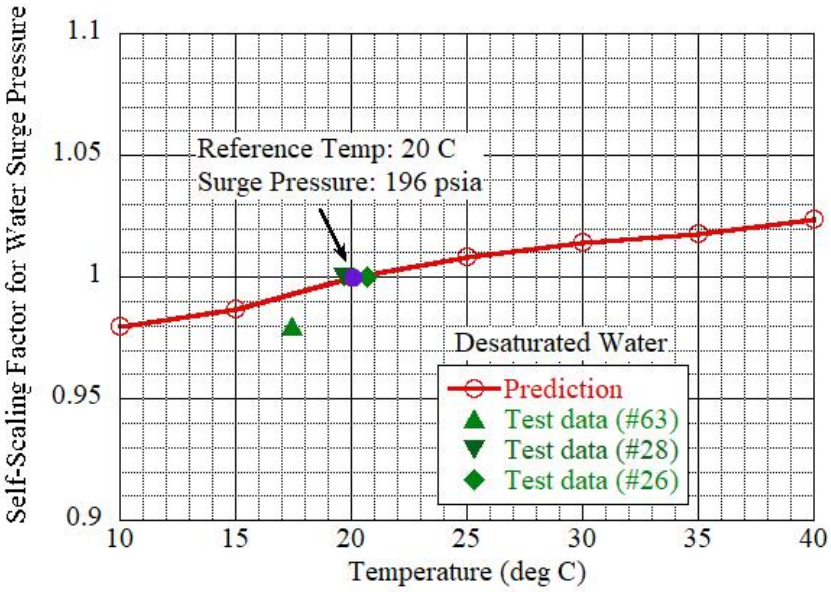

Fig. 5 Self-scaling scale factor for water surge pressure for desaturated water at a supply pressure of 150 psig.

The corresponding self-scaled surge pressure (absolute value) for water is presented in Fig. 6 for water surge pressure at 164.7 psia. As mentioned in the case of Fig. 5, the reference condition at 20 deg C is indicated by the purple dot, and the prediction is shown by the solid red curve. It appears that the self-scaled surge pressure in only weakly dependent on the inlet (supply) water temperature. The predicted surge pressure for water is within about 5 psia of the surge pressure at the reference temperature (20 deg C). At 10 deg C, the scaled surge pressure is 192 psia, which is 4 psia below the reference value of 196 psia. At 40 deg C, the scaled surge pressure is 192 psia, which is 5 psia above the reference value of 196 psia. This variation of 4 to 5 psia is within the range of uncertainty (1%) of the test setup pressure transducers (HPT, PT), which is 5 psi.

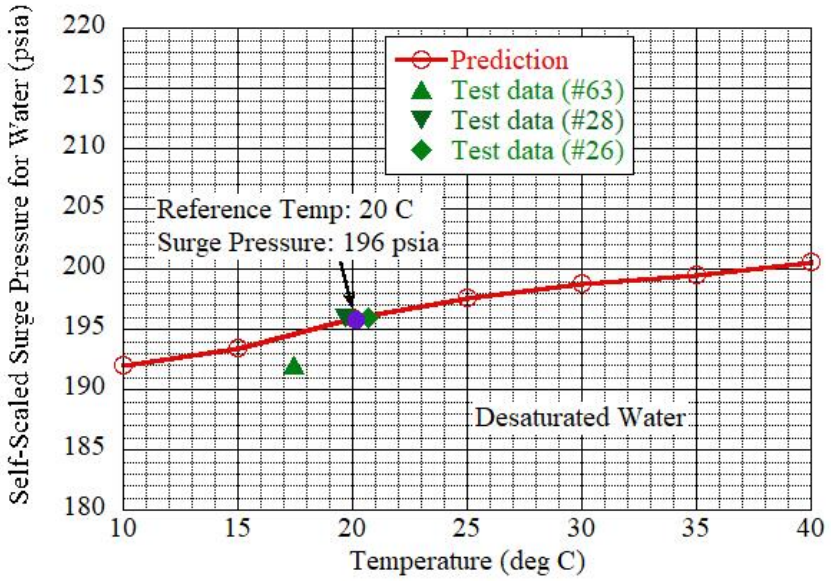

Fig. 6 Self-scaled surge pressure for water surge pressure for desaturated water at a supply pressure of 150 psig.

3. *Scaled Surge Pressure for Hypergols (Hydrazine, MMH, NTO)*

The scale factors from water to hypergols (hydrazine monopropellant along with MMH and NTO bipropellants) surge pressure as a function of supply temperature is depicted in Fig. 7. The fluid-to-fluid (water-to-hypergol) scale factor is determined based on Joukowsky equation (1b) and is assumed to be independent of the amount of the dissolved gas prior to priming. It is considered solely dependent on the density and speed of sound differences between the fluid. Note that the surge pressure for the saturated case is less than that for the desaturated for the same fluid depending on the amount of dissolved gas. The surge pressure scale factor from water to the three different propellants decreases nearly linearly with temperature. The scale factor for hydrazine decreases from about 1.4 at 10 deg C to about 1.26 at 40 deg C. The scale factors for MMH and NTO are successively lower than those of hydrazine. The predictions for MMH and NTO at 20 deg C supply satisfactorily agree with the data of Gibek and Maissoneuve[9] for a straight pipe. They are also assumed to be independent of inlet pressure.

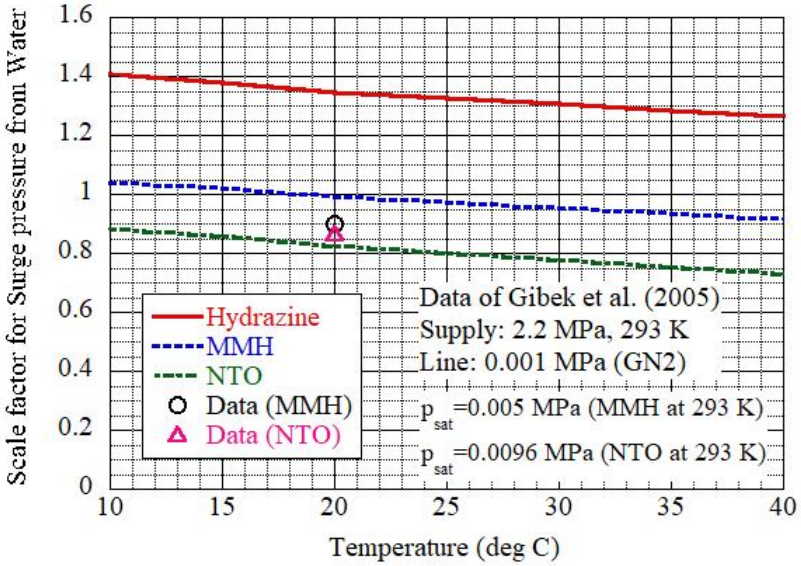

Fig. 7 Scale factor from water to hydrazine surge pressure

There is relatively little data for the ratio of surge pressures for desaturated and saturated cases at a given supply temperature. Our current tests with water show that at a temperature of 17.3 deg C, the ratio of desaturated to saturated surge pressures is 0.88. Data of Bombardier[2] for ethanol show that the corresponding ratio is also 0.88 at a temperature of 20 deg C. Unfortunately, there appears to be no data available for hypergols such as NTO, which can hold a relatively large amount of dissolved gas.

3. *Adiabatic Compression Temperature for Water*

Figure 8 shows a comparison of the adiabatic temperature rise for water surge at 150 psig supply. Calculations have been made for the adiabatic compression with a constant surge pressure (independent of initial temperature) and with a variable temperature-dependent surge pressure (based on self-scaling for water). The predicted temperature rise with a constant surge pressure is close to that obtained with scaled surge pressure. This is to be expected since for a given fluid the density and speed of sound changes with temperature are not appreciable. The predicted adiabatic temperature rise decreases slightly with increasing inlet temperature. It varies from about 2.1 deg C at 10 deg C inlet to about 1.6 deg C at 40 deg C inlet (constant surge). This level of temperature rise for the conditions considered here is fairly insignificant and is of the order of the measurement error (~0.5 deg C). Typically, the range of heater set points is higher than this adiabatic temperature rise. The predictions are somewhat higher than the test data by about 1 to 1.5 deg C. The measured tubing outer skin temperature rise is about 0.4 deg C, which is nearly independent of the supply temperature in a relatively narrow range of temperature (17 to 21 deg C).

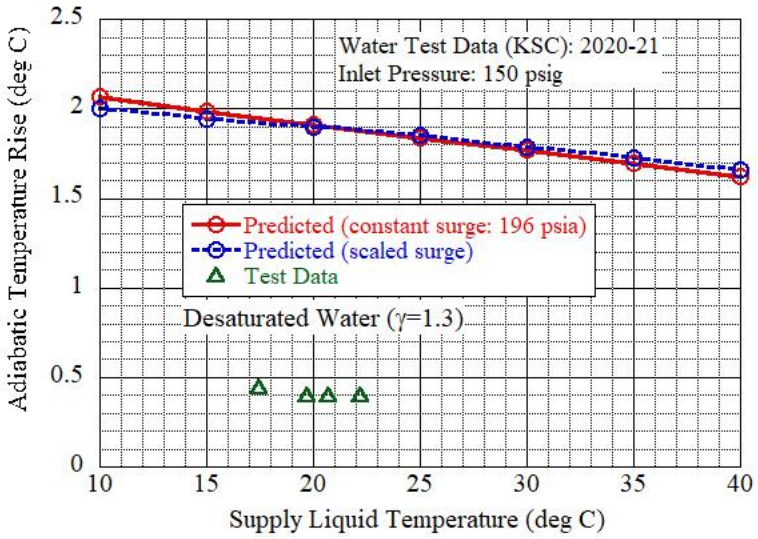

Fig. 8 Comparison of adiabatic temperature rise for desaturated water at a supply pressure of 150 psig.

The corresponding comparisons of adiabatic temperature for the desaturated water at 150 psig supply are indicated in Fig. 9. The predicted adiabatic temperature with a constant surge pressure is very close to that with scaled surge pressure (self-scaling) and increases linearly with the supply temperature. The predicted adiabatic temperatures are somewhat higher than the measured tubing skin temperature but appear to follow the same slope. The predicted adiabatic temperature for the desaturated and saturated cases at 150 psig supply lies within 1.5 deg C of the test data.

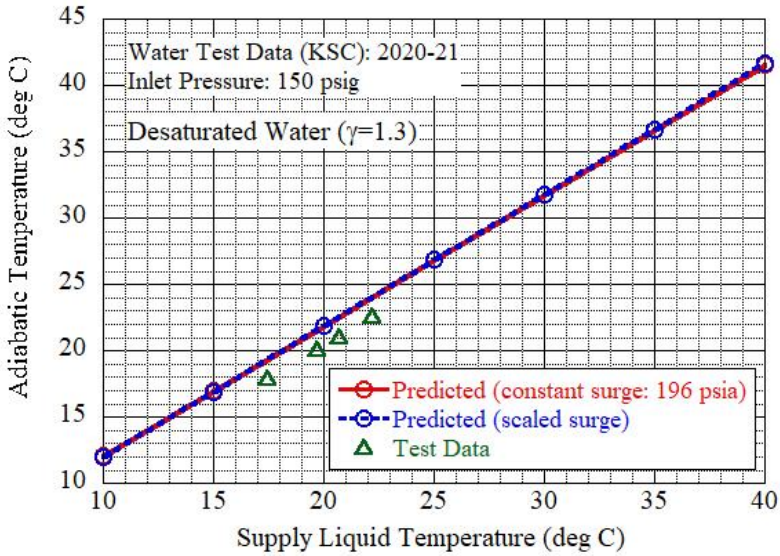

Fig. 9 Comparison of adiabatic temperature for desaturated water at a supply pressure of 150 psig.

The adiabatic temperature rise for water at 150 psig supply is compared in Fig. 10 for desaturated supply and for saturated supply at 150 psig inlet pressure. In both the cases, a constant surge pressure independent of the initial temperature is considered. The release of GHe in the case of saturated water (in addition to water vapor as in the desaturated case) results in a reduced surge relative to the desaturated case due to sound speed reduction in the two-phase mixture (according to Joukowsky equation). The theory shows that the adiabatic temperature rise during surge slightly decreases with an increase in supply temperature. The predicted temperature rise for saturated water is about 0.4 deg C higher relative to the desaturated case due to GHe release in close agreement with water test data. The

temperature rise agrees closely with the test data at 150 psig supply within 0.2 deg C. The liquid bulk temperature should be higher than the tubing skin temperature, and thus becomes closer to the prediction.

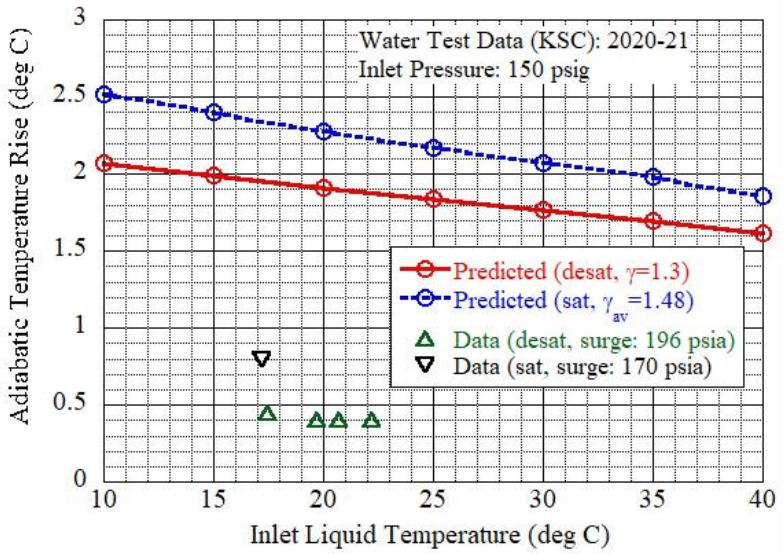

Fig. 10 Comparison of adiabatic temperature rise for desaturated and saturated water at a supply pressure of 150 psig.

Figure 11 presents the corresponding adiabatic temperature. Good agreement is noticed between the model predictions and the data for the adiabatic compression temperature. For water, the model predicts that the effect of saturation tends to increase the adiabatic compression by only about 0.4 deg C relative to the desaturated case, which is consistent with the temperature difference in the previously mentioned test data. The predicted adiabatic temperature for the desaturated and saturated cases at 150 psig supply lies within 1.5 deg C of the test data.

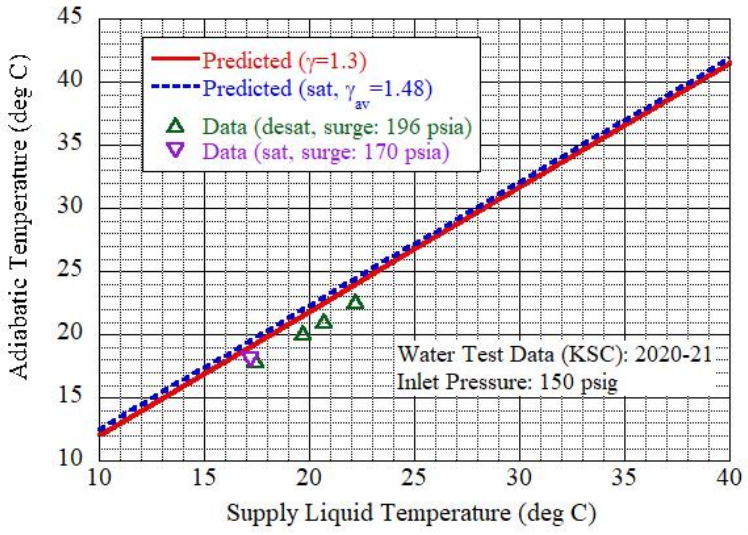

Fig. 11 Comparison of adiabatic temperature rise for desaturated and saturated water at a supply pressure of 150 psig.

C. Supply Pressure Effects on Surge Pressure and Adiabatic Compression

A comparison of the predicted surge pressure dependence on supply pressure with measurements for desaturated water is illustrated in Fig. 12. The measured surge pressure increases with supply pressure primarily due to increased flow velocity. It is seen that at increased supply pressure, the surge pressure deviates from linearity as indicated by the broken (purple) line. The predicted surge pressure slope with supply pressure (based on the Joukowsky equation) deviates considerably, although agreement is achieved near 200 psig supply. Other than pressure effects and uncertainties in the flow-cross sectional area, complex effects such as bends, branches, fittings, and the flex hose, not considered in the simplified Joukowsky model, could possibly explain the test-theory deviation (in surge pressure slopes). The model requires refinement in terms of appropriate correction factors.

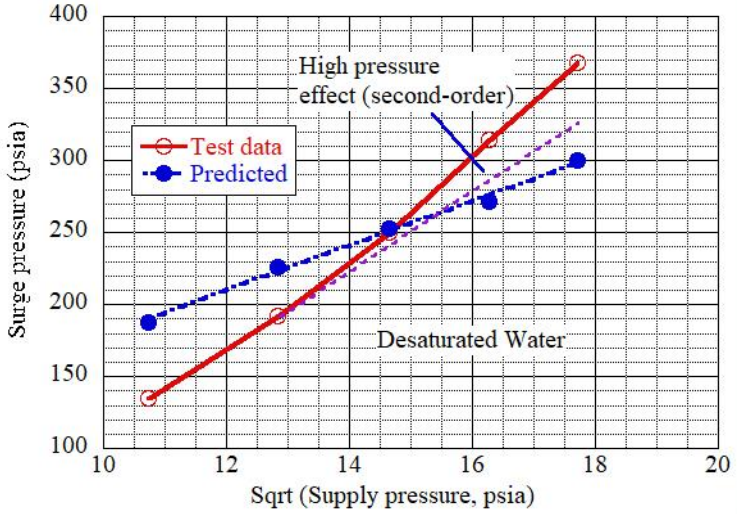

Fig. 12 Comparison of measured and predicted surge pressure dependence on supply pressure for desaturated water.

Figure 13 displays a corresponding comparison for the saturated water supply. The surge pressures for the saturated case are based on a scale factor of 0.88 applied to the predictions for the desaturated cases. Unfortunately, only two data points are available for comparison purposes. The main difficulty is that it takes several weeks to fully saturate the propellant with GHe in the current test setup with a 55-gallon supply tank and no mixing. The trends are similar to those seen for the desaturated case except that the surge pressure levels are smaller in the saturated case. As in the desaturated case, the model requires refinement in terms of correction factors for bends, flexhoses, etc.

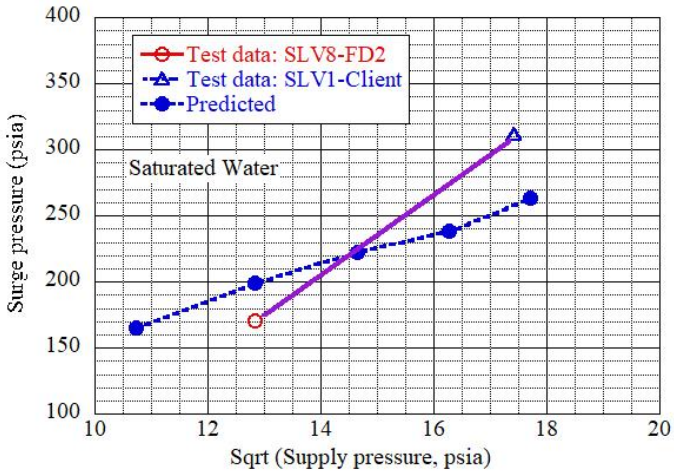

Fig. 13 Comparison of measured and predicted surge pressure dependence on supply pressure for saturated water

The dependence of adiabatic compression temperature rise on supply pressure for desaturated water, as predicted by the present model, is plotted in Fig. 14. In the measurements the inlet temperature varied from 15 to 20 deg C. The adiabatic temperature rise (based on the measured surge pressure) increases linearly with the supply pressure. It varies from 1.5 deg C at 100 psig supply to about 4 deg C rise at 300 psig supply. The test data show that the adiabatic temperature rise is nearly independent of the supply pressure (about 0.5 deg C), revealing conditions closer to an isothermal situation. These two curves probably represent the maximum and minimum bounds (adiabatic and isothermal limits) on the temperature rise. The actual temperature rise likely lies in between these two limits (which are only idealizations), and there is always some heat transfer during compression. Also, the complex effects of bends and flex hoses, not currently modeled, could partly explain the test-theory departure.

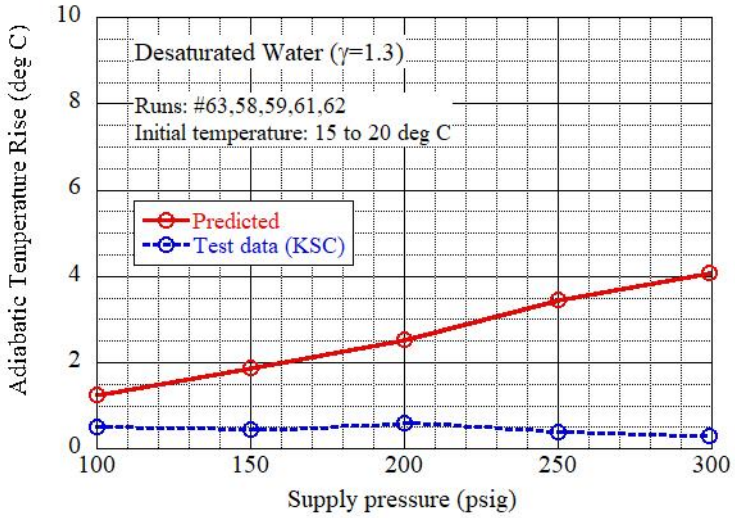

Fig. 14 Comparison of adiabatic temperature rise with supply pressure for desaturated water.

VI. Conclusions

The surge pressure is lower in a saturated liquid relative to a desaturated liquid. A scaling procedure has been followed for water-to-hydrazine (MMH, NTO) surge pressures based on Joukowsky equation, and for self-scaling (temperature-scaling) of water based on a reference temperature. The scaled surge pressure in water is relatively weakly dependent on the inlet temperature.

At 150 psig supply, the model predicts a 2 deg C adiabatic temperature rise for water at 10 deg C supply, linearly decreasing to about 1.5 deg C at 40 deg C supply. This prediction is somewhat higher than the measured tubing skin temperature For water, both the model and the data indicate that saturation of the supply liquid tends to increase the adiabatic temperature by about 0.4 deg C relative to the desaturated case as a result of GHe release during priming (even though the surge pressure for saturated water is about 30 psig lower at 150 psig supply).

The test data and model show that the surge pressure increases with increasing supply pressure. The predicted surge pressure dependence on the supply pressure reasonably agrees with the data in the supply range of 100 to 200 psig. At higher supply pressures, the data reveal a separate effect of supply pressure (superposed on the first-order flow velocity effect). This aspect (phenomenon) requires further investigation.

In general, the departure in surge pressure slope (in the surge pressure vs. square root of supply pressure map) between the theory and the data is likely due to the influence of the flex hose, bends, branches, etc., which were left out of account in the model based on the Joukowsky equation. The real value of the simplified Joukowsky equation is that it provided a sound scaling procedure for predicting hydrazine surge pressures in a flight application (considering its accuracy at 150 psig supply).

The predicted adiabatic temperature rise (based on the measured surge pressure) increases linearly with the supply pressure, while the test data show a weak dependence (near isothermal conditions). The model predicts an increase of 1.5 deg C at 10 deg C inlet and 4 deg C at 40 deg C inlet. The actual temperature rise is expected to lie between the adiabatic and isothermal limits, since these limits represent idealizations, and there is always some heat transfer during compression.

Further improvements and validations of the adiabatic compression model are required at higher surge pressures and elevated adiabatic compression temperatures. Also, the influence of the initial downstream line pressure on the surge pressure scaling needs to be investigated.

Appendix A: Model Validation with Existing Data

A-1 Ethanol/GN2 Priming

Figure A-1 shows the test data on adiabatic compression of ethanol/GN2 priming (Lecourt and Steelant[1]). Each curve in the plot corresponds to one experiment (run). The test section geometry is a 2 m long straight pipe (made of titanium alloy, TA3V) with 6.35 mm outer diameter and 0.41 mm wall thickness. Surge pressure (with an unsteady pressure transducer) and temperature (with a thermocouple protruded into the module cavity) were measured in a short measurement volume (40 mm long) near the end of the line (20 mm from the dead end). Data were acquired at a frequency of 40 Hz. The supply pressure is about 287 psia. The initial line pressure is 1.45 psia of GN2, and the initial liquid temperature is 5 deg C. The measured downstream surge pressure is about 23.1 MPa (3350 psia). With this level of surge pressure, the 40 Hz was likely insufficient, and several of the peaks were not captured. The instant $t = 0$ corresponds to the opening command of the (isolation) valve.

Considerable increase in GN2 temperature is attained due to surge compression on account of intense mixing between the liquid and GN2 in the narrow compression region. Consequently, there was a rise in liquid temperature of about 47 deg C (from an initial liquid temperature of 5 deg C to an equilibrium temperature of about 52 deg C) near the end of the line.

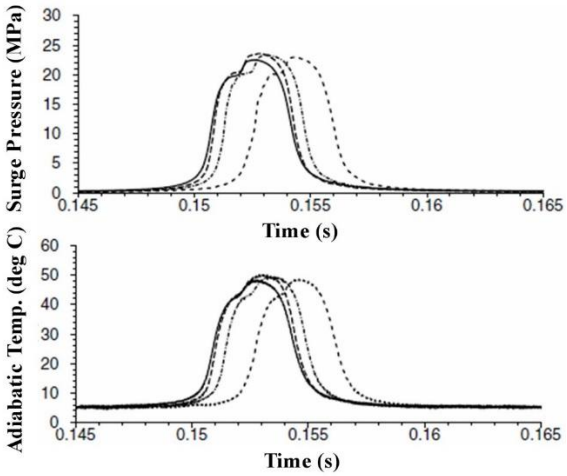

Fig. A-1 Test data on adiabatic compression for ethanol/GN2 priming.

Calculations based on the present model show that with the measured surge pressure (23 MPa), the present model predicts an adiabatic compression temperature rise of 64 deg C (final temperature of 69 deg C), which exceeds the measured liquid temperature increase of 47 deg C (final temperature of 52 deg C). At these surge levels, the compressed gas temperatures are relatively high so that heat losses (from the system to the surroundings) would be appreciable. Considering that the model does not account for heat losses during compression, the agreement between the prediction and the data may be considered satisfactory.

A-2 Liquid N2H4 (10% GN2+90% N2H4 Vapor)

Test data were obtained by Hutchinson and Schmitz[9] for GN2 and hydrazine mixture in the line. The test section is made of titanium tubing and fittings. Pressure and temperature transducers were located near the end of the line for measuring surge pressure and adiabatic temperature. Data for adiabatic compression of liquid N2H4 with the line containing 10% GN2 and 90% N2H4 vapor are presented in Fig. A-2. The supply pressure is 377 psia. With mostly hydrazine vapor in the line at 14.7 psia, the hydrazine temperature increased from 40 deg C to 60 deg C (temperature rise of 20 deg C). Increased initial line pressures tend to reduce the surge pressure. Based on the measured surge pressure of 882 psia and an initial line pressure of 14.5 psia, the present model predicts the equilibrium temperature of hydrazine as 57.3 deg C (temperature rise of 17 deg C). This prediction is quite close to the measured temperature of 60 deg C.

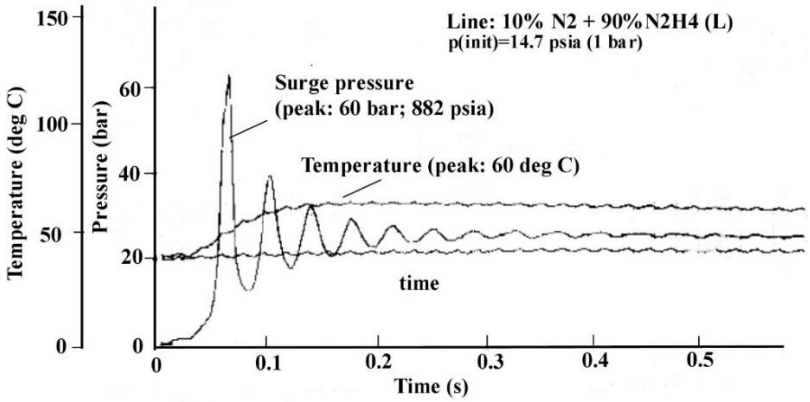

Fig. A-2 Test data on adiabatic compression for 10% GN2.

The measured surge pressure appears to be very high even though the line pressure is at ambient value providing considerable cushion initially. Achieving a high pressure peak that is about 2.3 times the initial pressure with a gas/vapor filled line may be possible in a dynamic pressure event with a fluid on both sides of a fast acting valve with a low pressure drop. This situation is quite different from the dynamics event with a nearly evacuated line of interest in our present study. There could likely be some hydrazine decomposition / thermal runaway that drove the pressure and temperature up and then it subsided after the cooler propellant was introduced. It is noteworthy that the test section did not explode under these circumstances. In fact, detonation did occur in a separate test with a supply pressure of 30 bar and temperature of 90 deg C, and the line filled mainly with hydrazine vapor. As the surge pressure was about 80 bar and the adiabatic compression reached 167 deg C, the test set up was detonated.

A-3 Liquid N2H4 – GN2

The measured surge pressures, obtained by Gibek et al.[10] for N2H4 priming with GN2 in the line, are displayed in Fig. A-3a. The corresponding data for adiabatic compression of liquid N2H4 are presented in Fig. A-3b. The test section is a 2 m long straight pipe (made up of TA3V), with an outer diameter of 6.35 mm and a thickness of 0.41 mm. At the downstream end of the test section, an instrumentation plug measures high frequency measurements of surge pressure and temperature. The supply conditions are 2.2 MPa (319 psia) and 293 K, and the line pressure is 0.1 MPa (14.7 psia). The measured peak surge pressure is about 2.7 MPa (392 psia). The measured peak hydrazine temperature rise is found to be 6 deg C. Based on the measured pressure of 2.7 MPa and an initial line pressure of 0.1 MPa, the present model predicts the equilibrium temperature rise of hydrazine as 2.2 deg C (equilibrium temperature of 22 deg C or 295 K). This prediction of 22 deg C for the equilibrium temperature is considerably lower than the measured peak equilibrium temperature of 26 deg C, but still considerably low from a safety point of view. Note that the peak temperature and the peak surge pressure occur at the first peak.

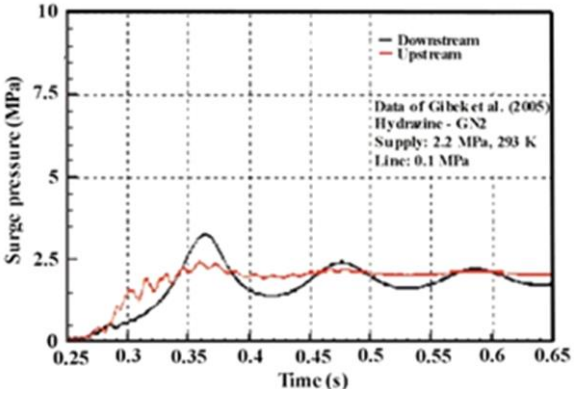

Fig. A-3a Test data on surge pressure for N2H4-GN2 system (Data of Gibek et al.[10]).

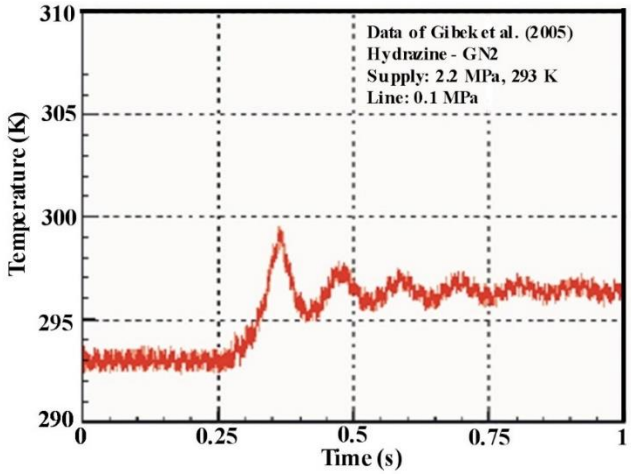

Fig. A-3b Test data on adiabatic temperature for N2H4-GN2 system (Data of Gibek et al.[10]).

The foregoing validations with existing data in the literature suggest that the current model for adiabatic compression compares well to some of these existing data sets at relatively low surge pressure, but there is appreciable departure at very high surge pressures. It is expected that at very high surge pressure, the trapped gas temperature can become very high, introducing large changes in temperature-dependent properties such as density and specific heat, so that the application (assumption) of an average temperature for the property evaluation can introduce considerable inaccuracy. Furthermore, heat losses from the system at elevated temperatures can be appreciable. Additional improvements to the model at elevated surge pressures are required. Nonetheless, in practical systems, the design surge pressures are kept below safety limits, so that the present model will be useful for prediction purposes.

Appendix B: Test Data on Surge Pressure and Adiabatic Compression

B-1 Surge Pressures

Figure B-1 displays the measured surge pressure history for Run #63 (dated 2-23-2021) with desaturated water, as measured by the low-speed (50 Hz data acquisition rate) pressure transducer (PT8) and the high-speed (5000 Hz data acquisition rate) pressure transducer (HPT5). At a supply pressure of 150 psig, the peak surge pressures indicated by the high-speed and low-speed pressure transducers during priming are about 192 psig and 190 psia respectively, showing very close agreement between the two measurements.

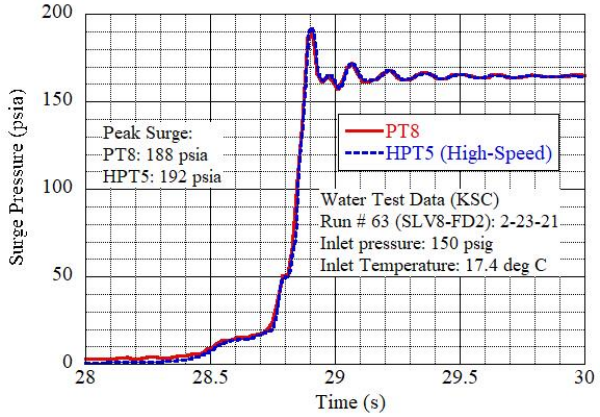

Fig. B-1 Measured surge pressure history in Run #63 for desaturated water at a supply pressure of 150 psig.

The measured adiabatic compression temperature as measured by the tubing skin and probe temperature history is shown in Fig. B-2. The adiabatic compression temperature level is roughly measured by a skin temperature sensor TT-15 mounted on the tubing. The bulk liquid temperature is measured by a probe TT-20, which indicates a lower peak temperature (and a lower temperature increase) due to adiabatic compression relative to TT-15 sensor.

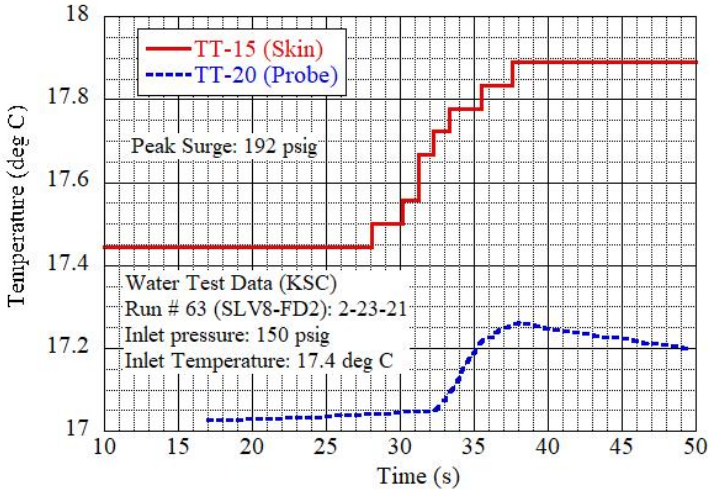

Fig. B-2 Measured adiabatic compression temperature history in Run #63 for desaturated water at a supply pressure of 150 psi.

Appendix C: Vapor Pressure Data for Water and Hydrazine

C-1 Vapor Pressure for Water and Hypergols (Hydrazine, MMH, NTO)

The vapor (or saturation) pressure curves for water is shown in Fig. C-1. For reference purposes, the vapor pressure curve for hydrazine (Schmidt[11]) is also included, along with those of MMH and NTO. It is seen that at a given temperature the vapor pressure is the highest for NTO, followed by MMH, hydrazine and water.

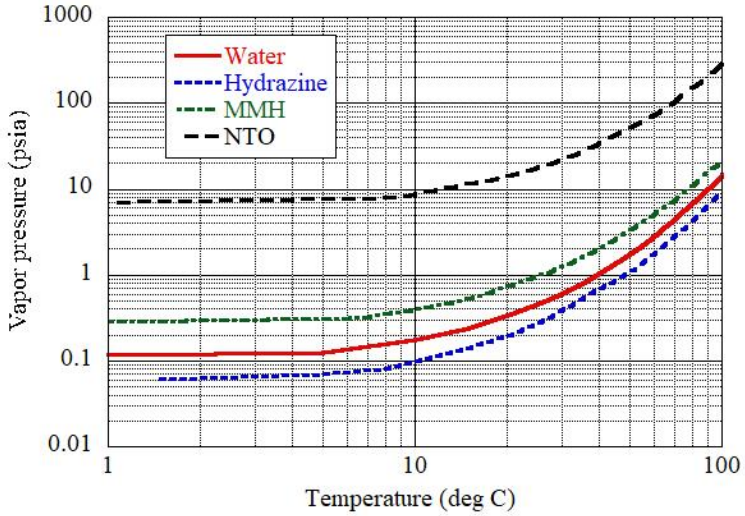

Fig. C-1 Vapor pressure curves for water and hypergols.

Acknowledgments

This work was funded by the NASA's Exploration and In-Space Services (NExIS) Division, Goddard Space Flight Center in cooperation with NASA Kennedy Space Center.

References

[1]Lecourt and Steelant, Experimental investigation of water hammer in simplified basic pipes of satellite propulsion systems, AIAA-2007-5532, 43rd AIAA/ASME/SAE/ASEE Joint Propulsion Conference, Cincinnati, Ohio, July 8-11, 2007.

[2]Bombardieri, C., Traudt, T., and Manfletti, C., Experimental study of water hammer pressure surge in spacecraft feedlines, 6th European Conference for Aerospace Sciences (EUCASS), Krakow, 2015.

[3]Velencia-Bel, F., Di Matteo, F., and van Meerbeeck, W., Assessment for hydrazine detonability during priming system activities, Space Propulsion Conference, Cologne, Germany, May 19-22, 2014.

[4]Espinosa, M., Webster, G.K., Coll, G.T., Nufer, B.M., Kandula, M., and Aranyos, T.J., Internal depressurization of hydrazine with application to in-orbit satellite refueling, AIAA-2018-3913, AIAA Joint Thermophysics and Heat transfer Conference, Atlanta, Georgia, 2018.

[5]Joukowsky, N.E., "On the hydraulic hammer in water supply pipes," *Memoirs of the Imperial Academy Society of St. Petersburg, 1898* (Russian to English Translation by O. Smith, Proc. Amer. Water Works Assoc., 1904, Vol. 24, pp. 341-424.

[6]Prickett, R.P., Mayer, E., and Hermel, J., Water hammer in a spacecraft propellant feed system, AIAA/ASME/SAE/ASEE 24th Joint Propulsion Conference, AIAA-88-2920, Boston, 1988.

[7]Scroggins, A.R., A streamline approach to venturi sizing, AIAA/ASME/SAE/ASEE 48th Joint Propulsion Conference, AIAA-2012-4028, Atlanta, 2012.

[8]Lema, M., Steelant, J., Pena, F.L., and Rambaud, P., Experimental characterization of the priming phase using a propellant line mock-up, Space Propulsion Conference, Bordeau, France, May 8, 2012.

[9]Hutchinson, F.E., and Schmitz, H.D., Adiabatic compression phenomena in hydrazine propulsion systems, AIAA/SAE/ASME 20th Joint Propulsion Conference, Cincinnati, Ohio, June 11-13, 1984.

[10]Gibek, I., and Maisonneuve, Y., Water hammer tests with real propellants, AIAA-2005-4081, 41st AIAA/ASME/SAE/ASEE Joint Propulsion Conference, July 10-13, 2005.

[11]Schmidt, E.W., *Hydrazine and Its Derivatives: Preparation, Properties, Applications*, 2nd ed., Vol. 1, John-Wiley & Sons, Inc., New York, 2001.